J Oceanogr (2011) 67:385–393
DOI 10.1007/s10872-011-0036-1

SPECIAL SECTION: ORIGINAL ARTICLE

Regional Environmental Oceanography in the South China Sea and Its Adjacent Areas (REO-SCS): I

# Source water of two-pronged northward flow in the southern Taiwan Strait in summer

**Huasheng Hong · Chen-Tung Arthur Chen · Yuwu Jiang · Jiann-Yuh Lou · Zhaozhang Chen · Jia Zhu**

Received: 1 September 2010 / Revised: 22 March 2011 / Accepted: 4 May 2011 / Published online: 5 July 2011


**Abstract** It is generally accepted that the flow is northward in the Taiwan Strait during summer and that the strongest current is detected in the Penghu Channel between the Penghu Islands and the Taiwan Island. This current, the eastern prong flow, is made up of waters from the South China Sea (SCS) and the Kuroshio. North of the Penghu Islands, the current veers to the west before turning northward again because of the shallow Chang-Yuen Ridge, and extends westward off the coast of Taiwan. There is a second prong of northward flow existing between the Taiwan Bank and the China mainland coast. Here, we show with observational data as well as results from a numerical model that this water receives little influence from the Kuroshio and is distinctively cooler, fresher, less oxygenated and more acidic, and contains more dissolved inorganic carbon than waters at the same density level of the eastern prong. Evidence is provided to show that the source water of the western prong should be the subsurface water from the strong upslope advection flowing northward from the SCS to the southern Taiwan Strait and upwelling along the coast during the favorable southwesterly wind. Subsequently, the upwelled water flows over the saddle west of the Taiwan Bank and joins the main flow northwest of the Penghu Islands.

**Keywords** Currents · Upwelling · Taiwan Strait · South China Sea · Source water · Hydrogeochemistry

H. Hong · Y. Jiang · Z. Chen · J. Zhu
State Key Laboratory of Marine Environmental Science, Xiamen University, Xiamen 361005, Fujian, China
e-mail: hshong@xmu.edu.cn

C.-T. A. Chen (✉)
Institute of Marine Geology and Chemistry, National Sun Yat-sen University, Kaohsiung 80424, Taiwan
e-mail: ctchen@mail.nsysu.edu.tw

J.-Y. Lou
Department of Marine Science, Naval Academy, Kaohsiung 81345, Taiwan

## 1 Introduction

The Taiwan Strait connects the East China Sea (ECS) and the South China Sea (SCS) and is approximately 180 km wide and 350 km long. The study of the Taiwan Strait is of interest because in winter the strong northeasterly monsoon induces strong southward flowing currents which flow along the coasts and transport fresher water as well as nutrients from the ECS to the SCS (Liu et al. 2000; Hong and Wang 2001; Jan et al. 2002; Chen 2008). In summer, the Kuroshio water may intrude into the northern SCS through the Luzon Strait, mixing with SCS waters and transporting saltier water from the SCS to the ECS. Part of the northward flowing water flows through the ECS and finally enters the Sea of Japan, carrying with it salt and other material, as well as heat (Fang et al. 1991; Isobe 2008).

The topography of the southern Taiwan Strait is shown in Fig. 1b. On the southeastern side is the funnel-like Penghu Channel which opens to the south and is over 200 m deep on the southern end. Because of the topography, it is well known that the deep Penghu Channel is the main pathway for the northward flow year long (Jan and Chao 2003). The neck of the channel east of the Penghu Islands shoals quickly to only 60 m. The shallow Chang-Yuen Ridge lies on the northern end of the neck (Fig. 1b), thus the subsurface flow is forced to turn westward and circumvent the ridge (Jan et al. 2002). There is a depression

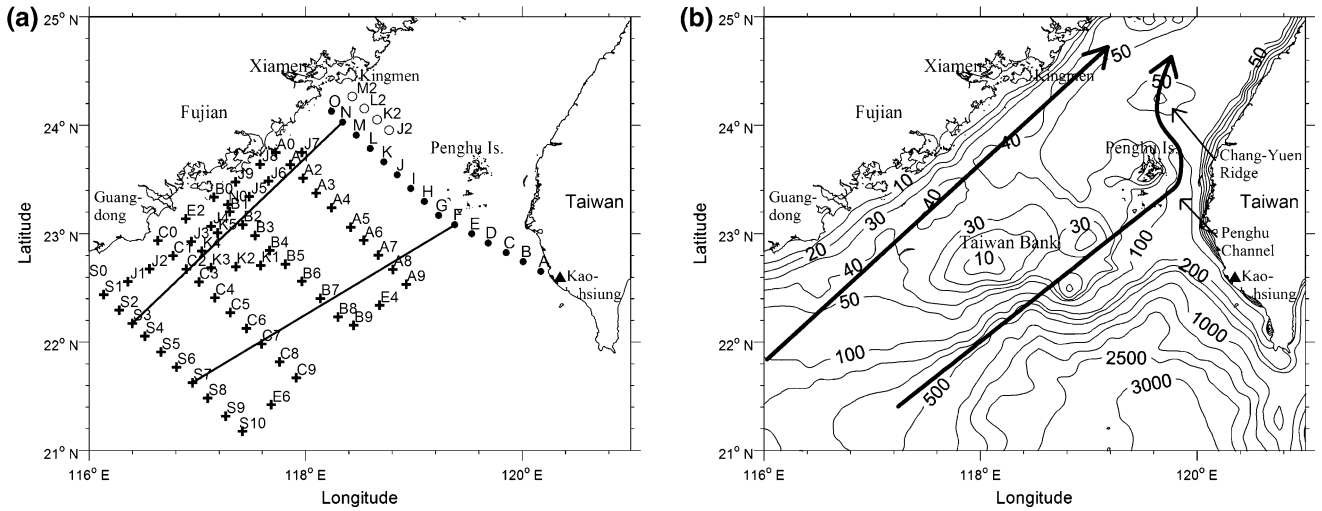


**Fig. 1** **a** Sampling stations during the three cruises in August 2001 (*filled circles*), May 2002 (*open circles*) and June–July 2006 (*plus symbols*). **b** Area studied with depth contours in meters. The two *solid lines* in (**a**) are the sections for presenting the results in Fig. 8. The two *arrows* in (**b**) schematically represent the two-pronged northward flow discussed in this paper

over 60 m in depth between the western end of the ridge and the coast of Fujian, so the flow naturally resumes its northward direction following this depression.

The middle part of the southern Taiwan Strait is the shallow Taiwan Bank which extends westward and is almost connected to the coast of eastern Guangdong. Because of the shallowness, subsurface flow here is expected to be weak. Nevertheless, between the Taiwan Bank and the coast of Fujian/Guangdong, there is also a northward flow (Hu and Liu 1992; Hu et al. 2000). The surface layer of the northward flowing western prong in summer contains much coastal water, including influences from the Pearl River plume (Hong et al. 2009). The source of the subsurface water is, however, less well known. It is the intention of this paper to show that the subsurface layer of the western prong is the upwelled SCS subsurface water, which has distinctively different properties compared to the main northward flow through the Penghu Channel. We limit our discussion to the subsurface waters below 10 m in water depth.

## 2 Sampling locations and methods

The authors conducted research cruises in the vicinity of the southern Taiwan Strait and northern SCS using the R/V "Ocean Researcher 3" (OR-III 721 cruise from 6 to 7 August 2001 and OR-III 776 cruise from 8 to 9 May 2002) and using the R/V "Yanping 2" during 20 June–2 July 2006. The relevant station locations are given in Fig. 1a. Temperature and salinity were determined with a shipboard SBE 911- or 917-plus conductivity–temperature–depth (CTD) unit manufactured by the Sea-Bird Corporation. The temperature was recorded on the International Temperature Scale and the salinity on the 1978 Practical Salinity Scale.

Discrete samples for the 2001 cruise were collected at various depths with a Rosette sampler fitted with 2.5-l Niskin bottles that were mounted on the Sea-Bird CTD unit for the determination of dissolved oxygen (DO), nitrate ($NO_3$), nitrite ($NO_2$), phosphate ($PO_4$), silicate ($SiO_2$), pH, and dissolved inorganic carbon (DIC). The sigma-$t$ ($\sigma_t$) was calculated based on the short form equation for the state of seawater (Chen and Millero 1977), and the apparent oxygen utilization (AOU) was calculated based on the oxygen solubility equation of Chen (1981). Details of the above are given in Chen and Wang (2006).

## 3 Hydrographical and geochemical data

Figure 2 shows the cross-section for potential temperature theta ($\theta$), salinity, $\sigma_t$, DO, AOU, $NO_3 + NO_2$, $PO_4$, $SiO_2$, pH and normalized DIC (NDIC = DIC × 35/salinity) during the OR-III 721 cruise. These properties are also plotted at the same density level in Fig. 3. The panels for $\theta$ (Figs. 2a and 3a) show very warm waters with temperatures as high as 30°C in the surface layer. In Fig. 2a, two low temperature domes are shown at Stn. G at the eastern tip of the Taiwan Bank and at Stn. M near the northwestern corner of the shoal. The one at Stn. G was easy to interpret as a mixture of the Kuroshio and the SCS subsurface waters creeping up the eastern flank of the Taiwan Bank when both wind and flow pointed northward at the time of the study. Figure 2b shows that the upwelling feature had higher salinity, which agrees with the hydrography in the region as there is an $S_{max}$ layer at around 100 m (Chen and

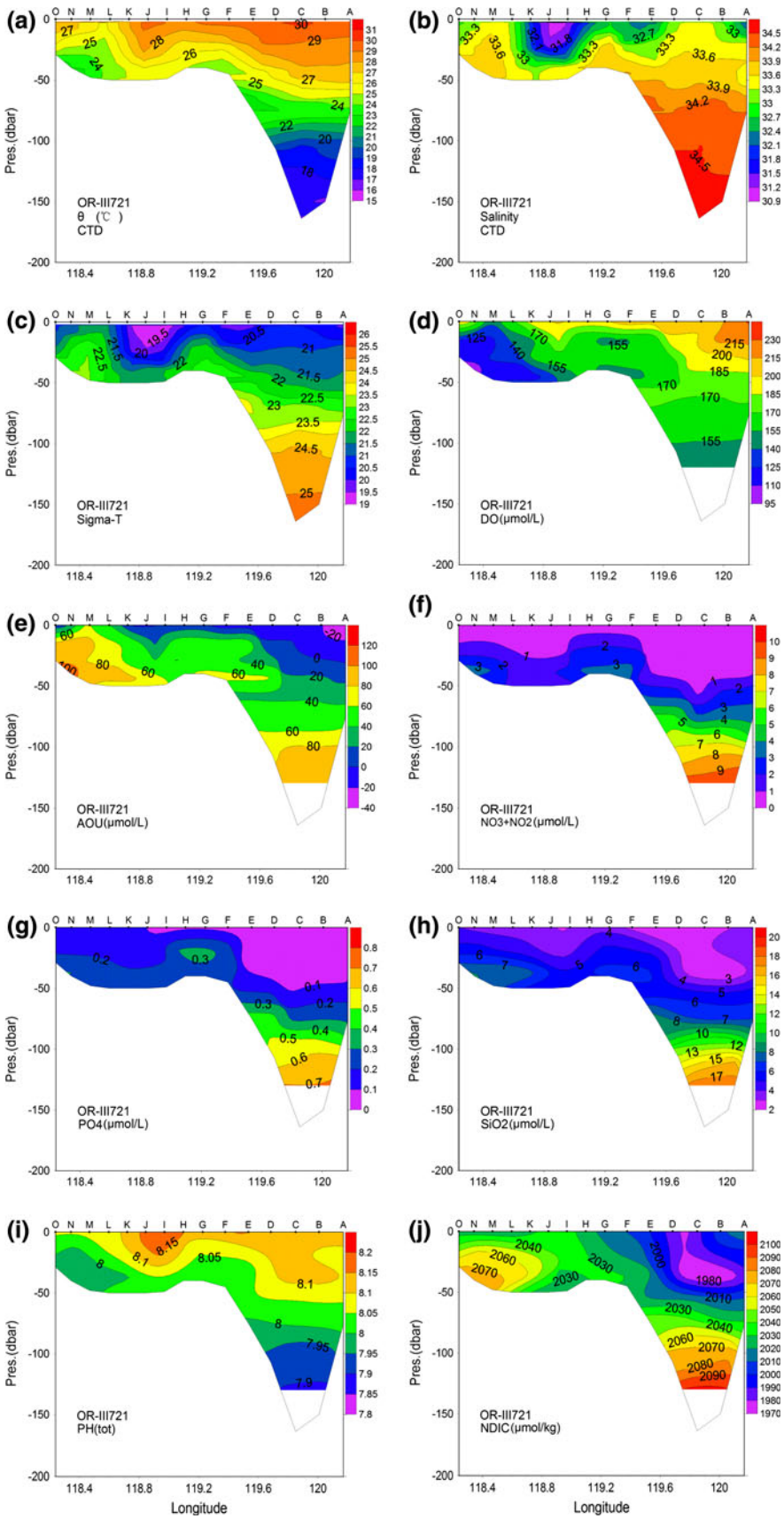


**Fig. 2** The cross-section for $\theta$ (**a**), salinity (**b**), sigma-*t* (**c**), DO (**d**), AOU (**e**), $NO_3 + NO_2$ (**f**), $PO_4$ (**g**), $SiO_2$ (**h**), pH (**i**) and normalized dissolved inorganic carbon (NDIC = DIC × 35/S) (**j**) during the OR-III 721 cruise (**a**, **b**, **d**, **e** modified from Naik and Chen 2008)

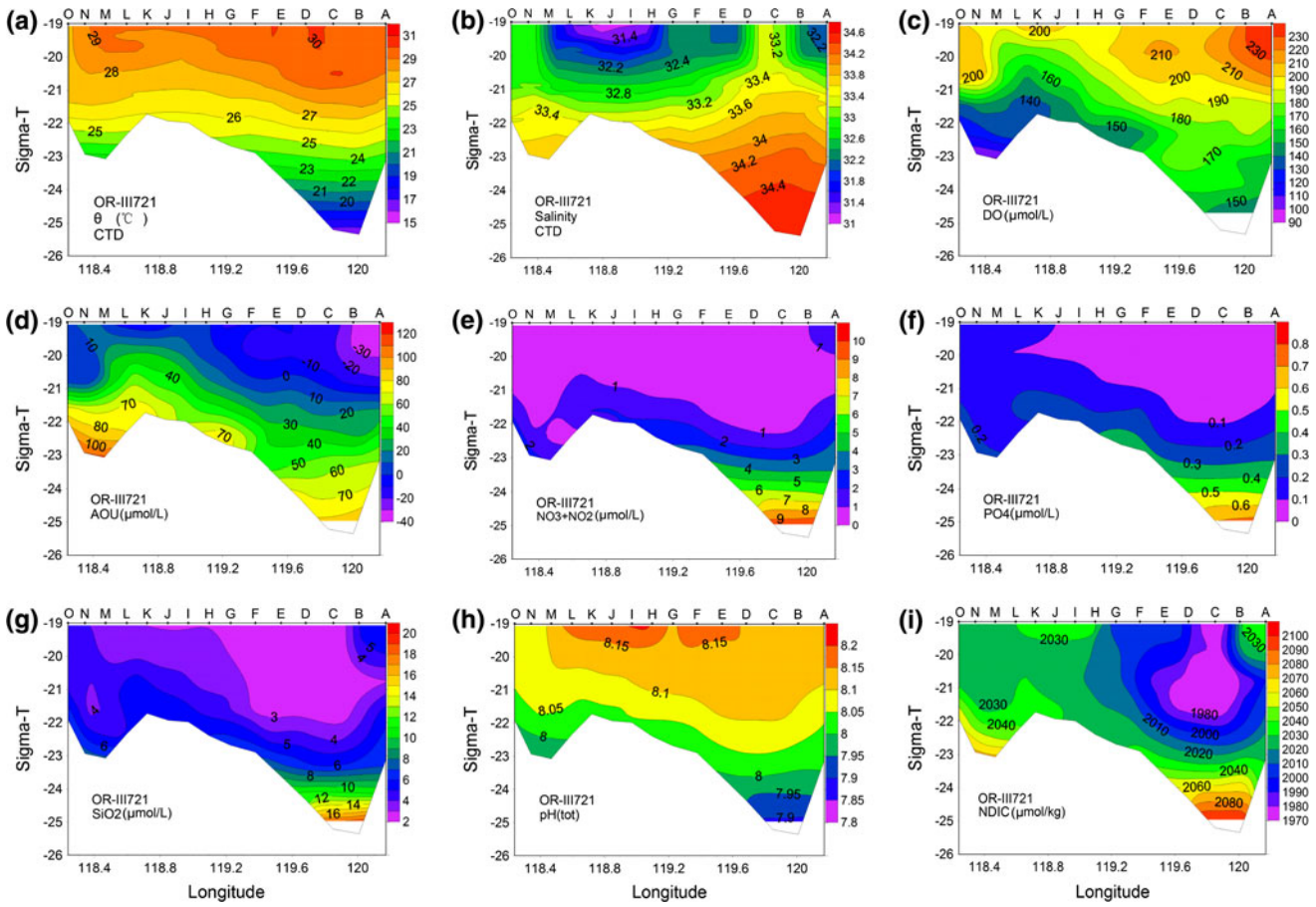


**Fig. 3** The $\sigma_t$ plotted versus $\theta$ (**a**), salinity (**b**), DO (**c**), AOU (**d**), $NO_3 + NO_2$ (**e**), $PO_4$ (**f**), $SiO_2$ (**g**), pH (**h**) and NDIC (**i**) during the OR-III 721 cruise

Huang 1996). This upwelling water had lower DO and pH, but higher AOU, nutrients and NDIC (Fig. 2d–j), all indicative of deeper waters. Because the upwelled waters move along the same density surface, the dome-shaped upwelling features at Stn. G do not show when plotted versus $\sigma_t$.

The low temperature but high salinity dome centered at Stn. M (Fig. 2a, b), however, is more difficult to explain. Our immediate guess was that it was part of the upwelling water from the Penghu Channel and was subsequently transported to where it was found. However, the temperature was more than 3°C lower than the upwelling water found on the western side of the Penghu Channel compared at the same depth. The DO of the bottom water at Stn. M was a full 60 μmol/L lower, and the AOU more than 60 μmol/L higher than the upwelling water at Stn. F (Fig. 2d, e). These low DO but high AOU features do not disappear when plotted versus $\sigma_t$ (Fig. 3c, d). Furthermore, the $\theta$–salinity plots for Stns. M and N west of the Taiwan Bank collected during the OR III-721 cruise were distinctively different from those at the other stations east of the Taiwan Bank (e.g., Stns. B, C, D, E; Fig. 4). These signatures do not support the idea that the water came from the extension of the upwelling water in the Penghu Channel (the $\theta$–salinity curves of Stns. B, C, D, E depart far from the curves of Stns. M, N in Fig. 4). Remnant winter water would have low temperature, DO and pH but high AOU, nutrients and NDIC (Naik and Chen 2008). But it may not be reasonable to expect the remnant winter water to stay for so long. It is worth noting that the $\theta$–salinity curves of waters of the western prong obtained during the 2002 and 2006 cruises also converge towards Stn. M (Fig. 4). Thus, it is clear that subsurface waters of the western prong have different properties compared with waters of the eastern prong.

Figure 5 shows the sectional distribution of temperature and salinity at three cross Taiwan Bank sections (A, B and C) during the R/V "Yanping 2" cruise in June–July 2006. The most distinguishable distribution was that there were two low temperature and high salinity zones in the lower layer separated by the Taiwan Bank. Such phenomena were quite distinctive in two sections (A and B). The temperature was lower on the western side of the Taiwan Bank than that on the eastern side, while the salinity

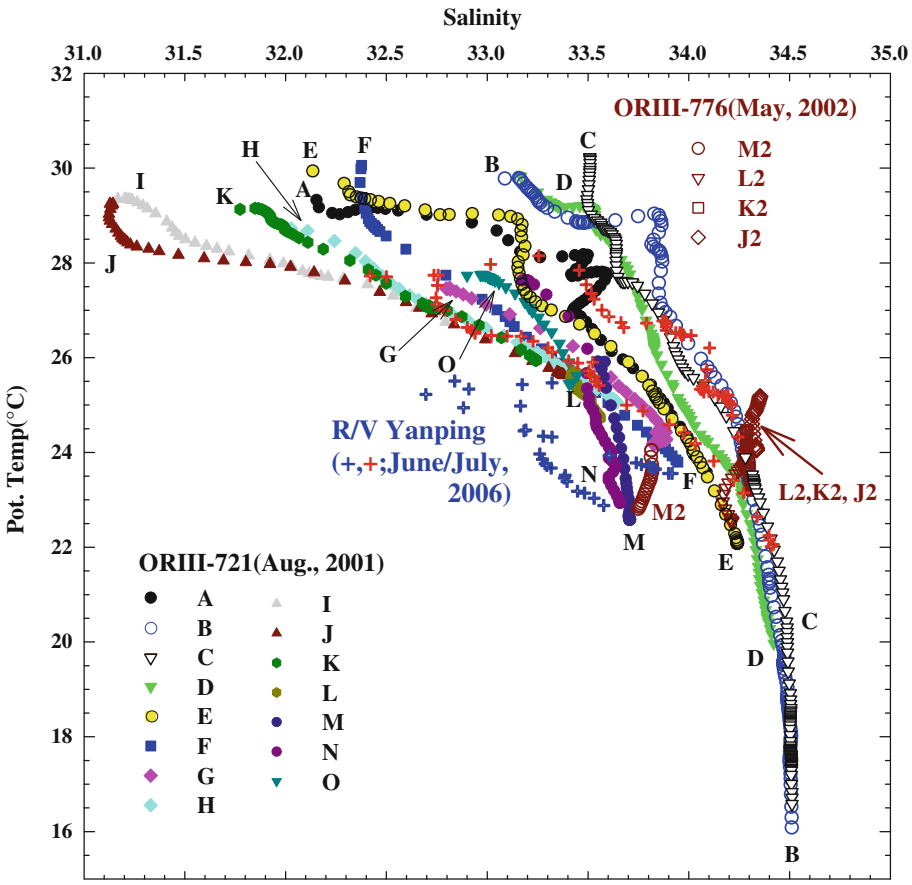


**Fig. 4** $\theta$–salinity plots of sampling stations during the OR-III 721, August 2001 (taken from Chen and Wang 2006); OR-III 776, May 2002; and Yanping 2 (*plus symbols*), June–July 2006 cruises. The $\theta$–salinity curves in the west of the Taiwan Bank (i.e. Stns. A2 and A3) are denoted with *blue plus signs* and those in the east of the Taiwan Bank (i.e. Stns. A8 and A9) with *red plus signs*

showed a slight difference between the western and eastern side. This pattern is similar to that observed in the OR-III 721 cruise (see Fig. 2a, b). In addition, both temperature and salinity were characterized by a stratified structure on both sides of the Taiwan Bank, but the hydrographical structure was vertically homogeneous over the Taiwan Bank (Fig. 5a–d).

The $\theta$–salinity curves of Section A during the R/V "Yanping 2" cruise are also plotted in Fig. 4. It is indicated that the $\theta$–salinity curves in the west of the Taiwan Bank (i.e. Stns. A2 and A3, + in blue) are quite different from those in the east of the Taiwan Bank (i.e. Stns. A8 and A9, + in red), again suggesting that the water mass at either side of the Taiwan Bank is not the same.

## 4 Modeling results

The existence of this two-pronged northward flow with different characteristics was further revealed by a high resolution model. The model was based on the Princeton Ocean Model (Mellor 2004), and a nest strategy was adopted in the modeling system. In the horizontal plane, the all-domain covered the Northwest Pacific with 1°/5°-coarse grids, and the sub-domain covered the Taiwan Strait with a 1°/25°-fine grid. In the vertical direction, there were 21 sigma levels. The fluxes at the air–sea interface were downloaded from the National Center for Environmental Prediction (Kalnay et al. 1996), and the boundary conditions were derived from the "Estimating the Circulation and Climate of the Ocean" project. The details of construction and verification of the model were given by Jiang (2007).

Figure 6 shows the cross-section for model salinity and temperature on 6 August 2001. The temperature and salinity were similar to the observed data shown in Fig. 2a, b. Two low temperature domes existed at the eastern tip of the Taiwan Bank and at the northwestern corner of the Bank, respectively. The corresponding salinity in these two domes was higher than that of the water above the Taiwan Bank. Results of the model circulation pattern (with the salinity and temperature distributions) on 6 August 2001 (Fig. 7a–d) show that there was a strong northward current from the SCS not only at 10 m depth but also at 25 m depth, so the cold water northwest of the Taiwan Bank cannot be from the north. The northward current in the 25-m layer was separated by the Taiwan Bank, where the main prong of the northward current flowing on the eastern side of the Taiwan Bank would be mixed with the Kuroshio water and flow through the Penghu Channel. However,

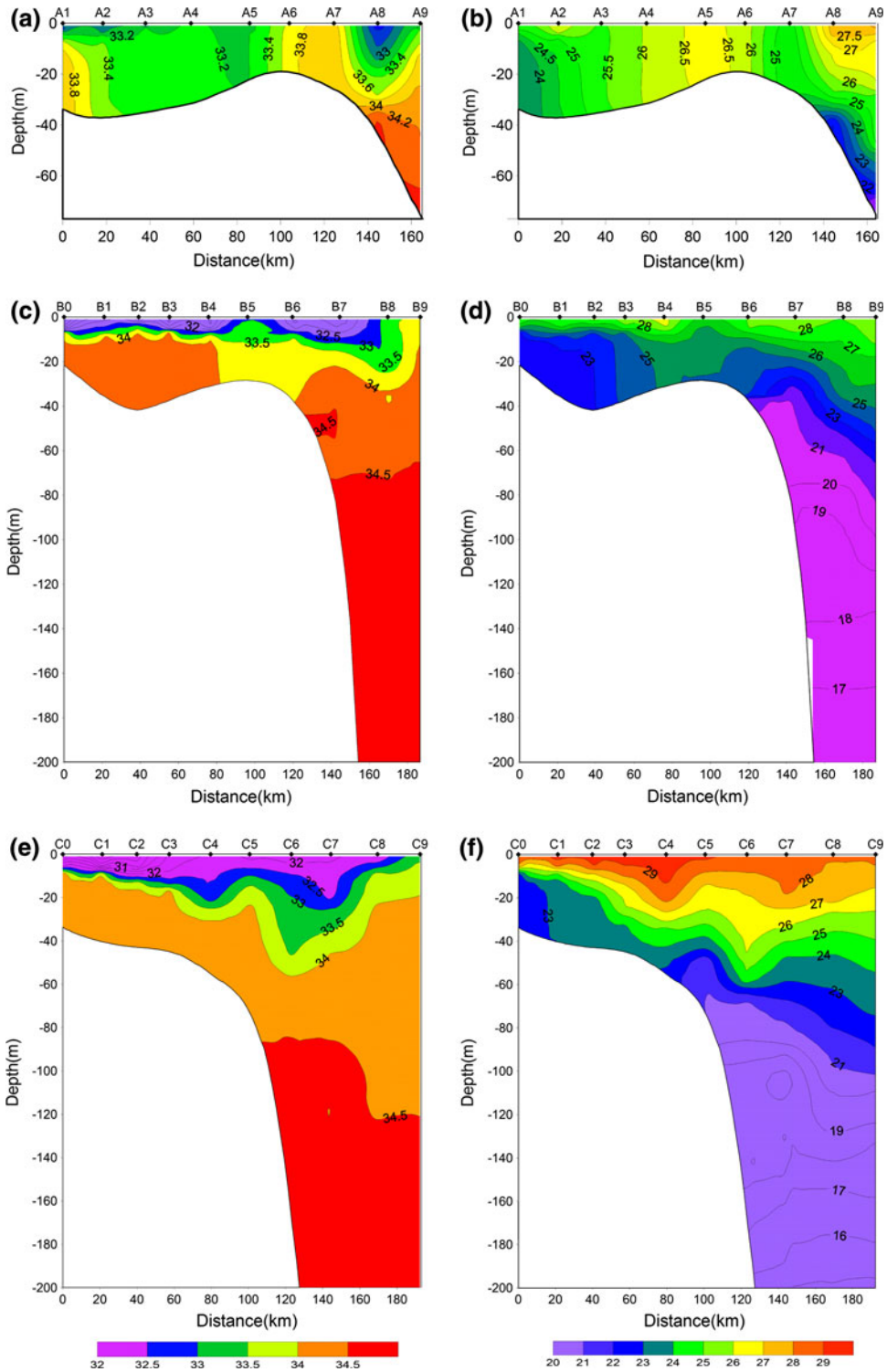


**Fig. 5** Sectional distributions of salinity (**a**, **c**, **e**) and temperature (**b**, **d**, **f**) during the cruise in June–July 2006. The *upper/middle/lower panels* are for Sections A/B/C, respectively

another prong of the northward current flowed on the western side of the Taiwan Bank and would receive little influence from the Kuroshio. This explains why the two prongs of the northward current, separated by the Taiwan Bank, have the distinctively different properties shown in Figs. 2a–j and 3c, d). The cold water east of Kingmen is shown to be connected with waters from the south (Fig. 7b). Some vertical mixing as the water flows over the hump west of the Taiwan Bank may explain why the water becomes warmer but less salty (Fig. 7b, d) north of the hump. Figure 7d now leaves the impression that the water north of the hump is isolated.

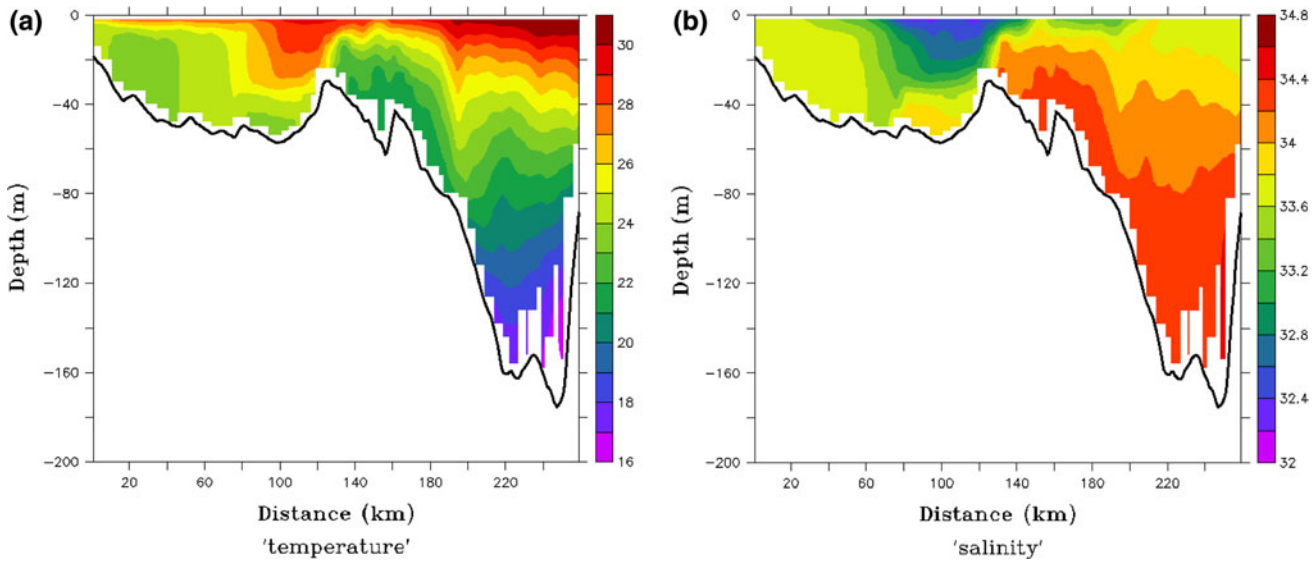


**Fig. 6** Model temperature (**a**) and salinity (**b**) in the section during the OR-III 721 cruise

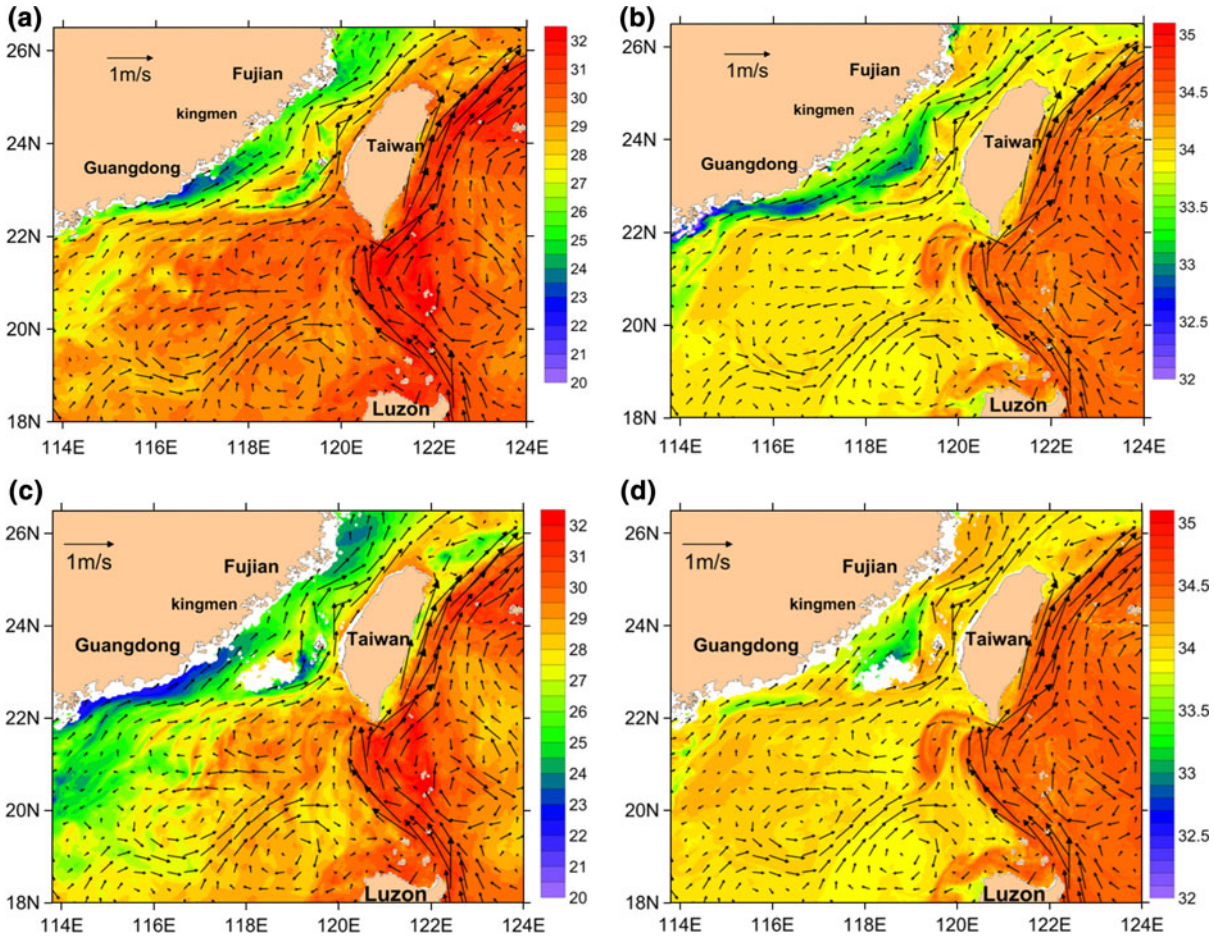


**Fig. 7** Model temperature and velocity in the 10-m (**a**) and 25-m layers (**c**); and model salinity and velocity in the 10-m (**b**) and 25-m layers (**d**) on 6 August 2001

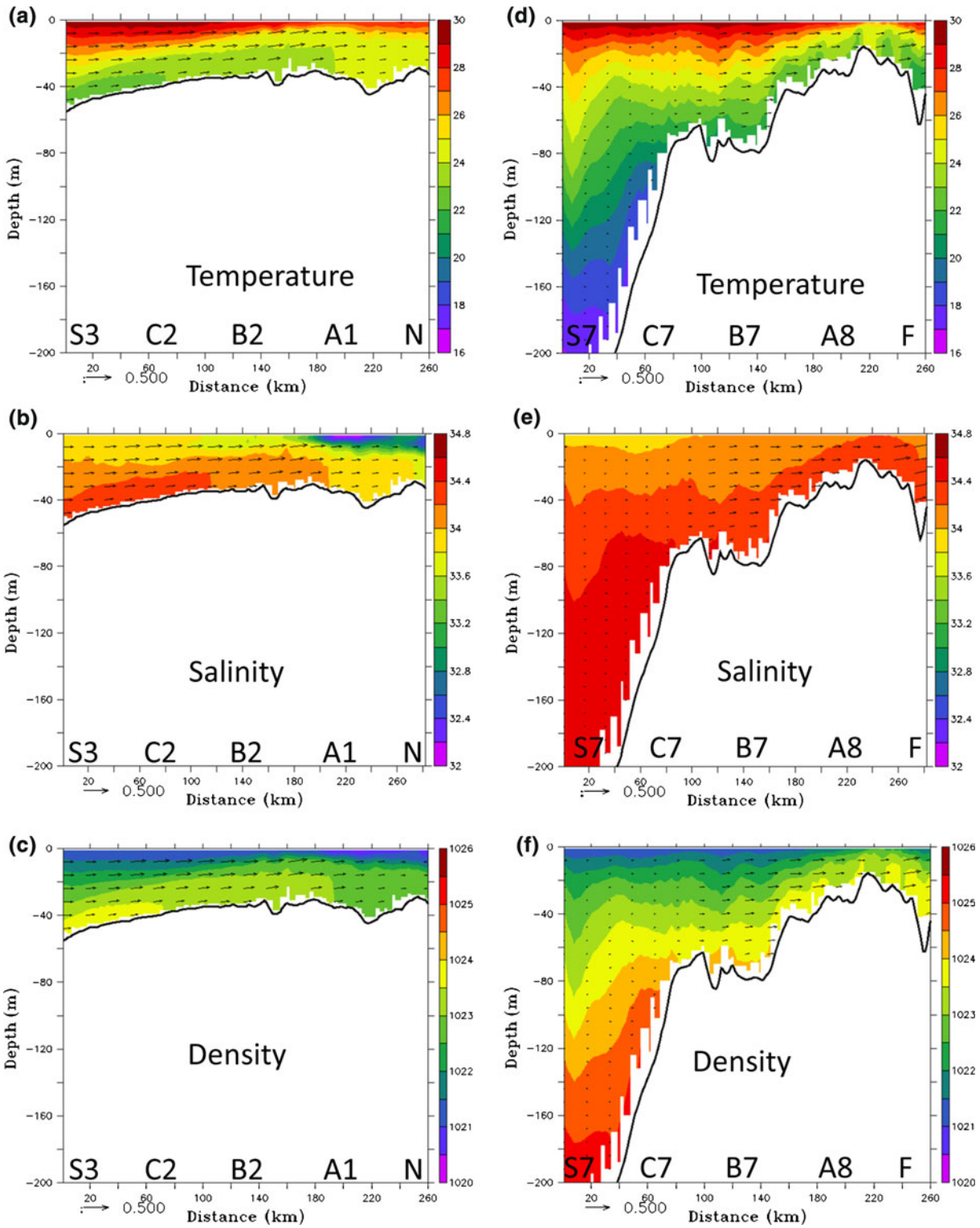


**Fig. 8** Sectional distributions of model temperature, salinity and density along Section S3-N (**a**–**c**) and along Section S7-F (**d**–**f**) on either side of the Taiwan Bank during the cruise observational period in June–July 2006. *Arrows* are currents from the numerical modeling. The section locations are shown in Fig. 1a

In order to determine the source of the water at either side of the Taiwan Bank, sectional temperature, salinity and density distributions at Sections S3-N and S7-F (see Fig. 1a for locations) were plotted from the corresponding numerical modeling results on 15 July 2006. As shown in Fig. 8a–c, both the 24°C iso-therm and the 34.2 iso-salinity

showed a tendency to climb northeastward along the section from the 35-m layer of Stn. S3 to the 15-m layer of Stn. B2, indicating the low temperature, high salinity and high density water comes from the subsurface layer of the northern SCS. Figure 8a–c also demonstrate that the current vectors directed northward along the section. As for the area east of the Taiwan Bank, it is clear from the distributions at the other section (Section S7-F) that the low temperature, high salinity and high density water, accompanied with northward current vectors, are climbing towards the upper layer of Stn. F near the Penghu Islands (Fig. 8d–f). However, the water property in Section S7-F may be affected by the Kuroshio's looping current because the Kuroshio is supposed to loop over the southern Taiwan Strait in summer (Fig. 7).

Bottom-mounted ADCPs also indicate that there is about a 15 cm/s northward current in all the column above the saddle in summer (Zhu et al. 2008), which can transport the subsurface water by strong upslope advection from the SCS to the Taiwan Strait, forming upwelling along the coast of Guangdong/Fujian during favorable southwesterly winds (Gan et al. 2009). Long-term measurement using high-frequency radar systems deployed near the coast of southern Fujian Province further indicate that there is a persisting northward current at a speed of about 10 cm/s in the western Taiwan Strait all year round (Zhu et al. 2008).

## 5 Conclusions

It has been known that the eastern prong of the northward flowing current in the Taiwan Strait in summer is made up of water from the SCS and the Kuroshio. Here, we have shown that strong upslope advection south of the Taiwan Bank brought up the SCS subsurface water. This water was subsequently transported over the saddle between the Taiwan Bank and the coast of Guangdong/Fujian Provinces, thus forming the western prong of the northward flowing current. This water received little influence from the Kuroshio and had distinctively different hydrographical and geochemical signatures from the Kuroshio water which flows northward along the Penghu Channel. Field observations and model simulations both indicated that the northward flow in the southern Taiwan Strait separated into two prongs by the Taiwan Bank is indeed coming from different sources.

**Acknowledgments** H.S. Hong's team would like to acknowledge the support from the NSFC Grant #40331004, #40810069004) and all the cruise members. C.T.A. Chen would like to acknowledge the financial support provided by the National Science Council of Taiwan (NSC 97-2621-M-110-002, 96-2628-M-110-002-MY3) and the Aim for the Top University Plan. Professor John Hodgkiss is thanked for polishing the English.

## References

Chen CT (1981) Oxygen solubility in seawater. In: Battino R (ed) Oxygen and ozone, vol 7. Pergamon, New York, pp 41–55

Chen CTA (2008) Distributions of nutrients in the East China Sea and the South China Sea connection. J Oceanogr 64(5):737–751. doi:10.1007/s10872-008-0062-9

Chen CTA, Huang MH (1996) A mid-depth front separating the South China Sea water and the West Philippine Sea water. J Oceanogr 52:17–25. doi:10.1007/BF02236530

Chen CT, Millero FJ (1977) Precise equation of state of seawater for the oceanic ranges of salinity, temperature and pressure. Deep Sea Res 24:365–369

Chen CTA, Wang SL (2006) A salinity front in the southern East China Sea separating the Chinese coastal and Taiwan Strait waters from Kuroshio waters. Con Shelf Res 26:1636–1653. doi:10.1016/j.csr.2006.05.003

Fang G, Zhao B, Zhu Y (1991) Water volume transport through the Taiwan Strait and the continental shelf of the East China Sea measured with current meters. In: Takano K (ed) Oceanography of Asian marginal seas. Elsevier, New York, pp 345–348

Gan JP, Li L, Wang DX, Guo XG (2009) Interaction of a river plume with coastal upwelling in the northeastern South China Sea. Con Shelf Res 29:728–740. doi:10.1016/j.csr.2008.12.002

Hong HS, Wang DZ (2001) Studies on biogeochemical process of biogenic elements in the Taiwan Strait. J Xiamen Univ 40(2):535–544 (in Chinese with English abstract)

Hong HS, Zheng QA, Hu JY et al (2009) Three-dimensional structure of a low salinity tongue in the southern Taiwan Strait observed in the summer of 2005. Acta Oceanol Sin 28(4):1–7

Hu JY, Liu MS (1992) The current structure during summer in southern Taiwan Strait. Trop Oceanol 11(4):42–47 (in Chinese with English abstract)

Hu JY, Kawamura H, Hong HS, Qi YQ (2000) A review on the currents in the South China Sea: seasonal circulation, South China Sea Warm Current and Kuroshio intrusion. J Oceanogr 56(6):607–624

Isobe A (2008) Recent advances in ocean-circulation research on the Yellow Sea and East China Sea shelves. J Oceanogr 64:569–584. doi:10.1007/s10872-008-0048-7

Jan S, Chao SY (2003) Seasonal variation of volume transport in the major inflow region of the Taiwan Strait: the Penghu Channel. Deep Sea Res II 50:1117–1126. doi:10.1016/S0967-0645(03)00013-4

Jan S, Wang J, Chern CS, Chao SY (2002) Seasonal variability of the circulation in the Taiwan Strait. J Mar Syst 35:249–268. doi:10.1016/S0924-7963(02)00130-6

Jiang YW (2007) The now-cast system for the current of the Taiwan Strait, a study of three-dimensional numerical model. Technical Report, State Key Laboratory of Marine Environmental Science, Xiamen University, Xiamen, Fujian, China, p 135

Kalnay E, Kanamitsu M, Kistler R et al (1996) The NCEP/NCAR 40-year reanalysis project. Bull Am Meteorol Soc 77(3):437–471

Liu KK, Tang TY, Gong GC et al (2000) Cross-shelf and along-shelf nutrient fluxes derived from flow fields and chemical hydrography observed in the southern East China Sea off northern Taiwan. Con Shelf Res 20:493–523. doi:10.1016/S0278-4343(99)00083-7

Mellor GL (2004) Users guide for a three-dimensional, primitive equation, numerical ocean model. Program in Atmospheric and Oceanic Sciences, Princeton University, Princeton.

Naik H, Chen CTA (2008) Biogeochemical cycling in the Taiwan Strait. Estuar Coast Shelf Sci 78:603–612. doi:10.1016/j.ecss.2008.02.004

Zhu DY, Li L, Li Y, Guo XG (2008) Seasonal variation of surface currents in the southwestern Taiwan Strait observed with HF radar. Chin Sci Bull 53:2385–2391. doi:10.1007/s11434-008-0207-7